Hindawi Publishing Corporation
EURASIP Journal on Applied Signal Processing
Volume 2006, Article ID 90716, Pages 1–9
DOI 10.1155/ASP/2006/90716

# Eigenspace-Based Motion Compensation for ISAR Target Imaging

**D. Yau, P. E. Berry, and B. Haywood**

*Electronic Warfare and Radar Division, Department of Defence, Defence Science and Technology Organisation (DSTO), Australian Government, Edinburgh, South Australia 5111, Australia*

Received 8 June 2005; Revised 17 October 2005; Accepted 24 November 2005

A novel motion compensation technique is presented for the purpose of forming focused ISAR images which exhibits the robustness of parametric methods but overcomes their convergence difficulties. Like the most commonly used parametric autofocus techniques in ISAR imaging (the image contrast maximization and entropy minimization methods) this is achieved by estimating a target's radial motion in order to correct for target scatterer range cell migration and phase error. Parametric methods generally suffer a major drawback, namely that their optimization algorithms often fail to converge to the optimal solution. This difficulty is overcome in the proposed method by employing a sequential approach to the optimization, estimating the radial motion of the target by means of a range profile cross-correlation, followed by a subspace-based technique involving singular value decomposition (SVD). This two-stage approach greatly simplifies the optimization process by allowing numerical searches to be implemented in solution spaces of reduced dimension.



## 1. INTRODUCTION

Imaging of targets using inverse synthetic aperture radar (ISAR) exploits the large effective aperture induced by the relative translational and rotational motion between radar and target and has the ability to create high-resolution images of moving targets from a large distance. The technique is independent of range if rotational motion is significant, and it therefore has good potential to support automatic target recognition. A target image is formed by estimating the locations of target scatterers in both range and cross-range but the scatterer motion needs to be compensated for in order to avoid image blurring which can occur due to scatterer migration between range cells and scatterer acceleration.

The common autofocusing methods can be categorized into parametric and nonparametric approaches. Computationally, nonparametric methods are much more efficient and easy to implement. The compensation for translational motion normally comprises two separate steps: range cell realignment and phase-error correction. Range cell realignment is considered to be routine and is based upon, for instance, the correlation method (see Chen and Andrews [1]) or the minimum-entropy method (see Wang and Bao [2]). Phase autofocus is more stringent in its requirements and many nonparametric methods have been proposed, most of which track the phase history of an isolated dominant scatterer (prominent point processing (PPP), see Steinberg [3]) or the centroid of multiple well-isolated scatterers (multiple scatterer algorithm (MSA), see Carrara et al. [4], Haywood and Evans [5], Wu et al. [6], Attia [7]). The phase-gradient algorithm (PGA, see Wahl et al. [8]) is another popular nonparametric technique, which iteratively estimates the residual phase by integrating over range an estimate of its derivative (gradient). Because nonparametric methods are based on the assumption of well-isolated dominant scatterers, they do not perform satisfactorily in many practical situations. On the other hand, parametric methods (Berizzi and Corsini [9], Xi et al. [10], Wu et al. [11], and Wang et al. [12]) are much more robust but more numerically intensive.

Common parametric techniques that use a polynomial model to approximate the target's translational motion and use an image focus criterion to estimate the model parameters are the image-contrast-based technique (ICBT, see [13]) and entropy-based technique (EBT, see [10, 14]). The challenge for autofocus is to devise algorithms which not only focus adequately for target recognition but are also both robust and efficient. This generally involves a tradeoff, between efficiency and effectiveness.

The nonlinear optimization techniques are employed to search for a solution for the parameters by optimizing the

image focus quality which is formulated as an objective function. Depending on the order of the model, the search is normally carried out over a two- or three-dimensional space. One major drawback of these methods is that the optimization algorithm (minimization/maximization routine or optimizer) often converges to a suboptimal solution if the objective function is highly multimodal or has a large number of local minima/maxima. Moreover, most deterministic optimization methods, such as Newton, gradient, and so forth, are constrained by the fact that the objective function has to be continuously differentiable.

In summary, a successful convergence to the optimal solution and the numerical efficiency of the method very much depend on various factors in relation to the nature of the objective function, such as differentiability and continuity, number of local minima/maxima, as well as the robustness of the optimization algorithm, for example its sensitivity to the initial guessed value.

The motion compensation technique described in this paper is a parametric method that does not depend upon the assumption of prominent scatterers but estimates the target's radial velocity based upon the composite of all of the target scatterers. It uses this to correct the data for the slant-range and cross-range phase errors due to the translational motion of the target, thereby significantly improving image quality.

In the proposed optimization procedure, the first-order and higher-order parameters of the target's radial motion are estimated sequentially by means of a range profile cross-correlation and a subspace-based technique involving eigendecomposition. By decoupling the first- and higher-order parameter searches, the technique allows the optimizers (minimization/maximization routines) to be implemented over spaces of lower dimension, and thus reduces the likelihood of converging to a suboptimal solution as encountered with other parametric methods. An overview of autofocus methods is given by Xi et al. [10] and Li et al. [14], and a recent survey is presented by Berizzi et al. [15].

## 2. PROBLEM FORMULATION

Consider a target with complex reflectivity function $\zeta(\mathbf{r})$ in the imaging plane of the target's frame of reference, that is, in slant-range $\hat{x}$ and cross-range $\hat{y}$ (see Figure 1). The target motion with respect to the radar line of sight (RLOS) can be decomposed into radial motion of an arbitrary reference point $O'$ on the target and rotational motion about the reference point. Let $R_0(t)$ denote the radial distance of $O'$ from the radar at time $t$ then $O'$ may be chosen to be the origin of the target's coordinate system (see Figure 1).

If the radial motion of the target's reference point $O'$ (due to translational motion) is defined by the initial velocity $v_{0r}$ and constant acceleration $a_r$, and if the target is rotating at an angular velocity of $\Omega$ about $O'$, then the distance from an arbitrary scatterer $(x_k, y_k)$ on the target to the radar at time $t$ can be written as

$$R_k(t) = R_0(t) + \Delta R_k(t), \tag{1}$$

where $R_0(t) = R_0(0) + v_{0r}t + a_r t^2/2$ and $\Delta R_k(t) = x_k \cos \Omega t - y_k \sin \Omega t$.

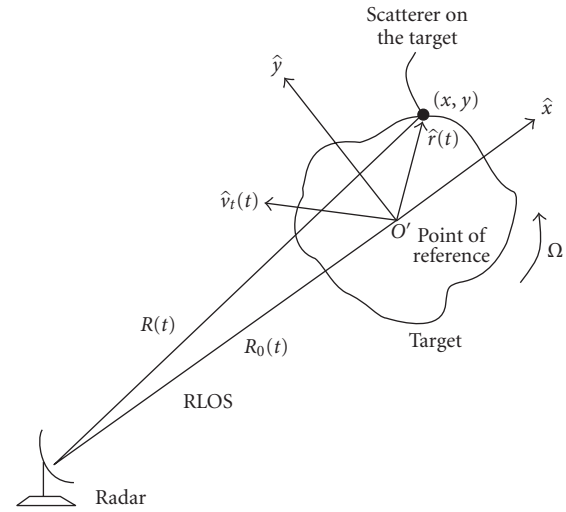


Figure 1: System geometry.

Let us define the transmitted RF signal for a coherent processing interval (CPI) of period $T$ as the real part of

$$z(t) = u(t)e^{2\pi j f_0 t}, \tag{2}$$

where $f_0$ is the carrier frequency and $u(t)$ is the complex envelope of the waveform given by $u(t) = A(t)\exp\{j\phi(t)\}$, and with Fourier transform $U(f)$, where $A(t)$ and $\phi(t)$ are the amplitude and phase modulation of the signal, respectively. Then the received signal after demodulation and downconversion to baseband can be written as

$$s_R(t) = \sum_{k=1}^{K} \zeta_k u(t - \tau_k(t)) \exp\{-j2\pi f_0 \tau_k(t)\}, \tag{3}$$

where $K$ is the number of scatterers on the target, $\zeta_k$ is the reflectivity of the $k$th scatterer which has local coordinates of $(x_k, y_k)$ with respect to $O'$ and is of distance $R_k(t)$ from the radar, $\tau_k(t)$ is the delay function given by $\tau_k(t) = 2R_k(t)/c$, and $c$ is the velocity of light.

If $\Omega$ is small in comparison to $T$ and the target's radial displacement is negligible for the duration of fast time sampling, then we can write the Fourier transform of the received signal as

$$S(f,t) = U(f) \sum_{k=1}^{K} \zeta_k \exp\{-2\pi j f \tau_k(t)\}, \tag{4}$$

where $t$ now refers to slow time, that is, pulse-to-pulse. The Fourier transform of the range profile, following the development in [9, 16], is therefore

$$S_R(f,t) = \frac{S(f,t)}{U(f)} = \sum_{k=1}^{K} \zeta_k \exp\{-2\pi j f \tau_k(t)\}. \tag{5}$$

Now $\tau_k(t) = 2R_k(t)/c = (2/c)[R_0(t) + \Delta R_k(t)]$, hence

$$S_R(f,t) = \exp\left\{-\frac{4\pi j f R_0(t)}{c}\right\} \sum_{k=1}^{K} \zeta_k \exp\left\{-\frac{4\pi j f \Delta R_k(t)}{c}\right\}, \tag{6}$$

where $\Delta R_k(t) \approx \hat{x}_k - \hat{y}_k \Omega t$, from which we see that phase changes occur in slow time for each scatterer but that the phase changes associated with radial target motion are separate from those associated with target rotation. The phase changes associated with the radial motion of the reference scatterer may therefore be corrected for by making the phase adjustment $4\pi j f R_0(t)/c$ to each pulse in the frequency domain. Since $R_0(t) = R_0(0) + v_{0r}t + a_r t^2/2$, we need to estimate $v_{0r}$ and $a_r$ for the reference scatterer.

The corrected range profile Fourier transform is then

$$S'_R(f,t) = \exp\left\{\frac{4\pi j f R_0(t)}{c}\right\} S_R(f,t) = \sum_{k=1}^{K} \zeta_k \exp\left\{-\frac{4\pi j f \Delta R_k(t)}{c}\right\}, \tag{7}$$

from which the realigned and phase-compensated range profile may be recovered by means of an inverse FT. Frequency estimation may then be performed in each range cell for cross-range velocity estimation. In a radar system, $f$ and $t$ take the digitized forms of $f = f_m$ $(m = 1,\ldots,M)$ and $t = pT$ $(p = 1,\ldots,N)$, where $f_m$ is the $m$th sample in the frequency domain and $T$ is the pulse repetition interval (PRI); $M$ and $N$ are the number of frequency samples and Doppler pulses, respectively.

The radial motion of the target has the effect of causing scatterers to migrate between range cells, and hence smearing of the image in the range dimension; whereas the $1/2a_r t^2$ term alone causes nonlinear phase variation in slow time, and hence smearing of the image in the cross-range dimension. If the length of the burst is sufficiently small compared with the rotation rate of the target, then the $y_k \Omega t$ term is approximately linear and provides the Doppler information necessary for cross-range imaging.

## 3. VELOCITY AND ACCELERATION CORRECTION TECHNIQUE

The purpose of the present paper is to estimate the radial velocity and acceleration so as to determine the delay $\tau$ and hence correct for the phase in the data. The optimization procedure comprises maximizing the objective functions $F_v(\overline{v}_{0r})$ and $F_a(a_r)$ separately for the single variable $\overline{v}_{0r}$ and $\overline{a}_r$ spaces, respectively, whilst keeping the other motion parameter fixed. The objective functions are formulated in a way such that $F_v(\overline{v}_{0r})/F_a(a_r)$ is relatively invariant to the changes of the fixed parameter $a_r/\overline{v}_{0r}$. This not only allows the optimization to be implemented solely in one-dimensional space, but also guarantees a fast convergence rate. The two-stage estimation technique procedure is summarized in Figure 2 and as follows: initial estimation of velocity using a cross-correlation technique followed by estimation of acceleration using a subspace-based approach. Further refinement is achieved as required by repeating the previous steps although in practice, at most only three iterations are required.

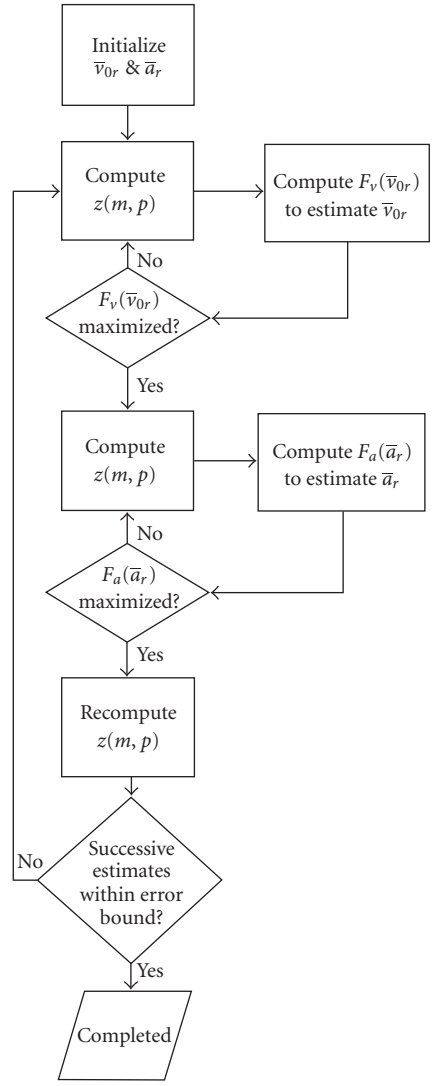


FIGURE 2: Flowchart showing the procedure for estimating velocity and acceleration.

Denote the matrix of complex radar signals organized according to range cell and pulse, respectively, by $z(m,p)$. For assumed values of $\overline{v}_{0r}$ and $\overline{a}_r$, the previously described procedure for range realignment and phase compensation is applied to the recorded data of (6) . The range profile $z(m,p)$ produced for range cells $m = 1,\ldots,M$ and Doppler pulses $p = 1,\ldots,N$ is written as the inverse discrete Fourier transform of (6) after being adjusted for phase errors as follows:

$$z(m,p) = \mathrm{IDFT}\left[\xi(\overline{v}_{0r},\overline{a}_{0r},pT)S_R(f_m,pT)\right], \tag{8}$$

where $\xi(\overline{v}_{0r},\overline{a}_{0r},p) = \exp\{-j4\pi f \overline{R}_0(\overline{v}_{0r},\overline{a}_{0r},pT)/c\}$ is the term associated with phase compensation of the received

data, and $\overline{R}_0$ is the corresponding radial range displacement of the target at time $t = pT$ given some estimates of velocity and acceleration $(\overline{v}_{0r}, \overline{a}_{0r})$. In the following, it is shown how the objective functions are formulated separately in terms of the parameters $\overline{v}_{0r}$ and $\overline{a}_{0r}$ for optimization.

The measure of how well the range realignment and phase compensation have been achieved is to compute the cross-correlation function $r_{1,p}(0)$ between the first range profile (i.e., for the first pulse) and each of the remaining range profiles, and summing their moduli, thus

$$F_v(\overline{v}_{0r}) = \sum_{p=2}^{N} |r_{1,p}(0)|, \tag{9}$$

where $r_{1,p}(0) = \sum_{m=1}^{M} z^*(m,1)z(m,p)$. The velocity estimate is that value of $\overline{v}_{0r}$ (given the correct $\overline{a}_{0r}$) which maximizes the objective function $F_v(\overline{v}_{0r})$, either by a blind search procedure or by formal optimization.

Following the improvement in the estimate of $\overline{v}_{0r}$, the range realignment and phase compensation procedure are repeated. The acceleration $\overline{a}_r$ is estimated as follows. The acceleration estimation technique exploits the fact that there will be many scatterers within the range cells occupied by the target to be imaged, which have a very similar radial velocity, although there will be a relatively small spread due to the superimposed varying cross-range rotational velocities. Because we are concerned with estimating a radial velocity which changes within the duration of a burst, we take a fixed window within which it is assumed that the radial velocity is approximately constant and fit a linear model to all of the range cells. This produces a covariance matrix which is averaged over range cells. This has the advantage of incorporating all of the energy from the target's scatterers rather than having to find and depend upon one of a small number of prominent scatterers. As a general criterion for spectral estimation techniques, the size of a fixed window of pulses should be chosen to be greater than or equal to the size of the signal subspace.

A data matrix is constructed from range profiles taken within a window superimposed on the pulses in slow time, thus

$$\mathbf{Z}_i = \begin{bmatrix} z(1,n_i) & \cdots & z(1,n_i+N_d-1) \\ \vdots & \ddots & \vdots \\ z(M,n_i) & \cdots & z(M,n_i+N_d-1) \end{bmatrix}, \tag{10}$$

where the window begins with the $n_i$th pulse and contains $N_d$ pulses. Then the covariance matrix $\mathbf{R}_i = (1/M)\mathbf{Z}_i^H\mathbf{Z}_i$ for the $i$th window is formed by averaging over the range cells. Subspace theory tells us that the principal eigenvectors span the same subspace as the signal vectors. In general, we will not know the dimensions of these subspaces (except that their sum is $N_d$), but it is sufficient for our purposes to identify the dominant signals associated with the signal subspace through eigendecomposition.

Therefore, the covariance matrix is subject to the eigendecomposition

$$\mathbf{R}_i = \mathbf{V}_i\Lambda_i\mathbf{V}_i^H, \tag{11}$$

where the $\Lambda_i = \mathrm{diag}(\lambda_1, \lambda_2, \ldots, \lambda_{N_d})$ is the diagonal matrix of eigenvalues with $\lambda_1 \geq \lambda_2 \geq \cdots \geq \lambda_{N_d}$ and $\mathbf{V}_i = [\mathbf{v}_{i,1}\ \mathbf{v}_{i,2}\ \cdots\ \mathbf{v}_{i,N_d}]$ is the matrix containing all the corresponding eigenvectors.

Computationally, singular value decomposition (SVD) is a more practical approach to computing the set of eigenvectors directly from the data matrix $\mathbf{Z}_i = \mathbf{U}_i\Sigma_i\mathbf{V}_i^H$, where $\mathbf{U}_i$ is an $M$-by-$M$ unitary matrix, $\Sigma_i$ is a diagonal matrix of the form $\Lambda_i = \mathrm{diag}(\sigma_1, \sigma_2, \ldots, \sigma_{N_d})$, and $\sigma_k(1, \ldots, N_d)$ are the singular values which are related to the eigenvalues by $\lambda_k = \sigma_k^2$. The diagonal matrix $\Sigma_i$ $(\Lambda_i)$ is always full rank because of receiver noise. The noise power is small in comparison to the signal power, and thus the signal subspace can be determined by examining the singular values.

The assumption behind the method is that the principal eigenvectors contain the Doppler information for the dominant scatterers on the target for the $i$th window. All of the scatterers will be subject to phase changes between pulses: one component will be a linear phase shift due to the common initial velocity $v_{0r}$ and the other nonlinear phase shift due to acceleration $a_r$. This may be seen from the range response function $\zeta_0 e^{-4\pi j f_0/c(R_0+v_{0r}t+1/2a_rt^2)}$ for the reference scatterer. The Doppler information implicit in two data matrices taken from different time intervals, say $Z_i$ and $Z_{i+j}$, will differ by an amount proportional to the change in the velocity or acceleration $a_r$. In mathematical terms, this difference corresponds to the "rotation" of the signal subspace with respect to the origin of the vector space. However, when the acceleration has been correctly adjusted, the signal subspace or the principal eigenvectors associated with the windows should coincide (within an arbitrary phase).

We suppose that only two windows are chosen. A measure of how well the principal eigenvectors coincide between the first and second windows of the burst is the sum of the moduli of their respective inner products:

$$F_a(\overline{a}_r) = \sum_{k=1}^{N_p} |\mathbf{v}_{1,k}^H\mathbf{v}_{2,k}|, \tag{12}$$

where $N_p$ is the number of principal eigenvectors chosen to represent the signal subspace. This objective function $F_a(\overline{a}_r)$ is to be maximized over $\overline{a}_r$. For simplicity, we choose the eigenvector which corresponds to the largest eigenvalue for each window so that $F_a(\overline{a}_r) = |\mathbf{v}_{11}^H\mathbf{v}_{21}|$. In fact, the number of windows chosen is arbitrary and is always a compromise between accuracy and efficiency. For example, if we choose $N_w$ windows and use the first window as the reference, then the objective function is reformulated as $F_a(\overline{a}_r) = \sum_{i=1}^{N_w} |\mathbf{v}_{11}^H\mathbf{v}_{i1}|$.

It can be easily shown that the number of computer operations required for calculating $F_v(\overline{v}_{0r})$ is $M(N-1)$ and for $F_a(\overline{a}_r)$ is approximately $4MN_p^2 - 4N_p^3/3$ (the number of operation required for SVD).

## 4. RESULTS

A summary of the radar parameters used in the simulation is given in Table 1 and a diagram showing the configuration of point scatterers on the test target is displayed in Figure 3. The reflectivity of the scatterers is indicated by the size of

Table 1: Radar parameters.

| | |
|---|---|
| Pulse compression | Stepped frequency |
| Number of sweeps | 64 |
| Number of transmitted frequencies | 64 |
| Centre frequency | 10 GHz |
| Frequency step | 2.34 MHz |
| Bandwidth | 150 MHz |
| PRF | 74.46 kHz |

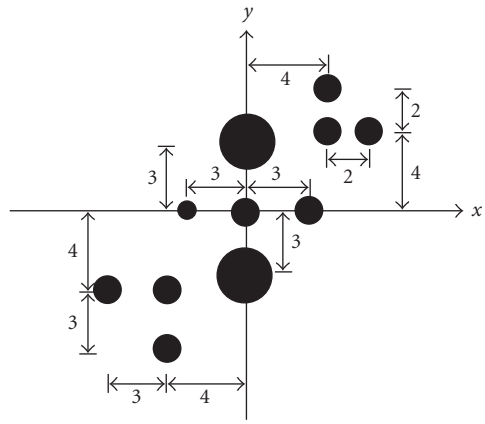


Figure 3: Simulated target point reflector configuration.

the circles in the drawing. The relative sizes are 0.5, 1 and 2, respectively. The target is travelling towards the radar with an initial velocity of 5 m/s and with constant acceleration of 2 m/s$^2$, with self-induced rotation of $0.16\pi$ rad/s.

Our technique is compared to Haywood-Evans MSA [5] and PGA [8] motion compensation techniques with a signal-to-noise ratio (SNR) of 20 dB. The results are shown in Figure 4 and it can be seen that the present technique generates a better focused image than the other techniques. Using our technique, $v_{0r}$ and $a_r$ are estimated to be 5.15 m/s and 2 m/s$^2$, respectively. For a detailed examination of the behavior of the objective functions, $F_v$ and $F_a$ are plotted against $v_{0r}$ and $a_r$ in Figures 5(a) and 5(b). The objective functions are also plotted with respect to fixed parameters in Figures 6(a) and 6(b). It can be seen that their variation is relatively insignificant as compared to the previous figures. Another similar set of data but with lower signal-to-noise ratio (SNR = 10 dB) was tested and used for comparison between the different techniques. The resulting images are shown in Figure 7. Again our technique outperforms MSA and PGA.

In computing these plots, the subspace technique was implemented using two windows of size 8. Only the eigenvector which corresponds to the largest eigenvalue was used to maximize $F_a(a_r)$. The computation time taken was less than 1 second on a Pentium IV 2.5 GHz computer and took roughly 10 times longer than the PGA method. This is comparable to the ICBT and EBT methods as stated in [15]. The algorithm was run on Matlab and the maximization was implemented by a toolbox function called *fminbnd* (used to minimize the negative of the objective functions). It took only two iterations for the optimization algorithm (Figure 2) to converge to the desired results. On average, it required about 10 iterations for *fminbnd* to maximize each objective function.

Next, we show an experimental example of a Boeing 737 (Figure 8) ISAR image reconstructed using MSA and the proposed subspace algorithm in Figure 9. The radar is at ground level and the parameters are lowest frequency = 9.26 GHz, frequency step = 1.5 MHz, range resolution = 0.78 m, PRF/sweep rate = 20 kHz/156.25 Hz; and the size of the data matrix is 64 by 64. Again it is seen that the proposed technique produces a much better image.

## 5. CONCLUSIONS

This paper has proposed a new parametric autofocus method for simultaneously realigning range and compensating for phase by estimating radial velocity and acceleration using a combination of range profile correlation for velocity estimation and subspace eigenvector rotation for acceleration estimation. The method does not suffer from the limitation of assuming the existence of prominent scatterers as in other nonparametric methods.

As shown in the paper, by formulating the objective functions with respect to only a single variable and implementing the optimization in two separate steps, the problem of convergence to a suboptimal solution suffered by other parametric methods can be avoided. It has proven to be both robust and has demonstrated that good results can be achieved in terms of image quality.

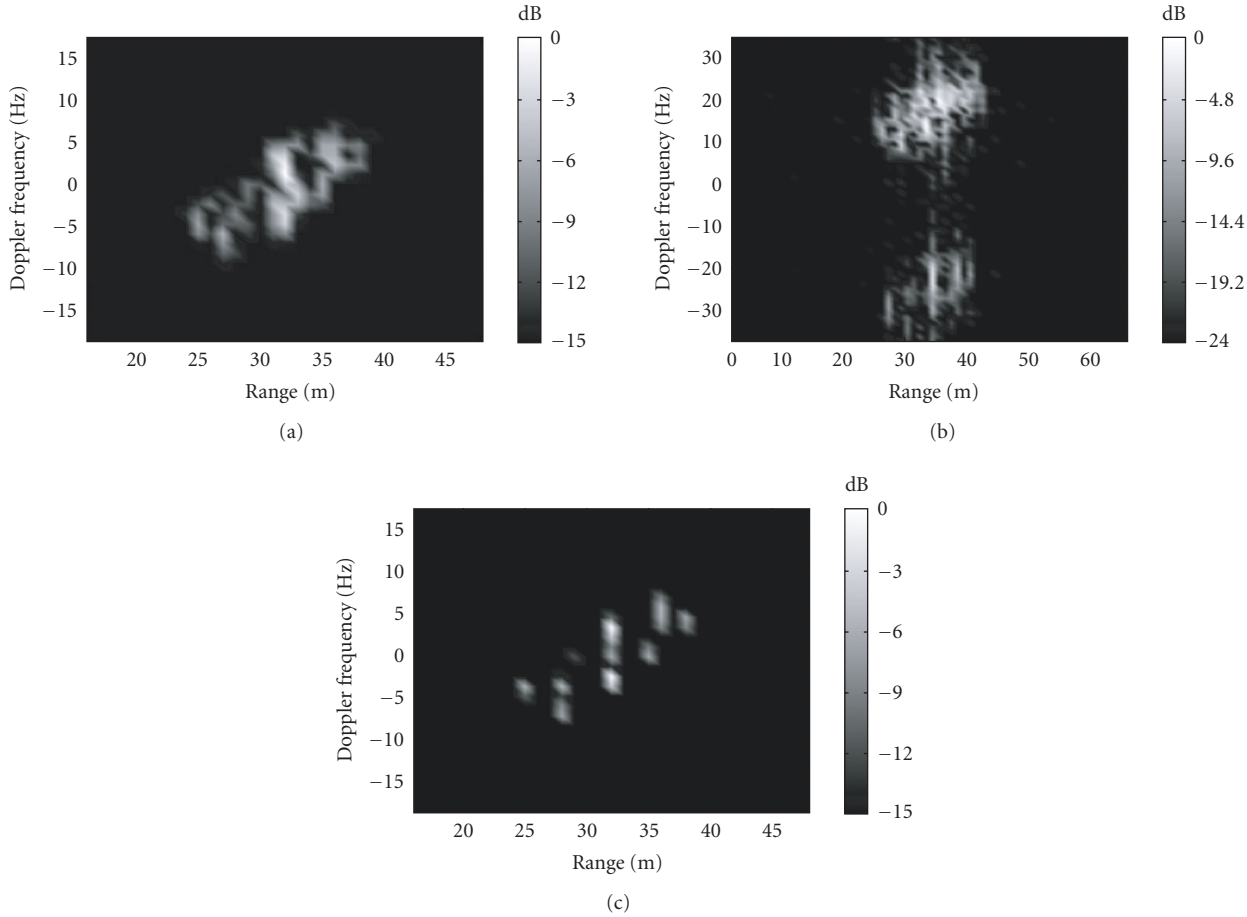


Figure 4: Range-Doppler image of simulated target (SNR = 20) using (a) MSA technique [5]; (b) PGA technique [8]; (c) proposed subspace technique.

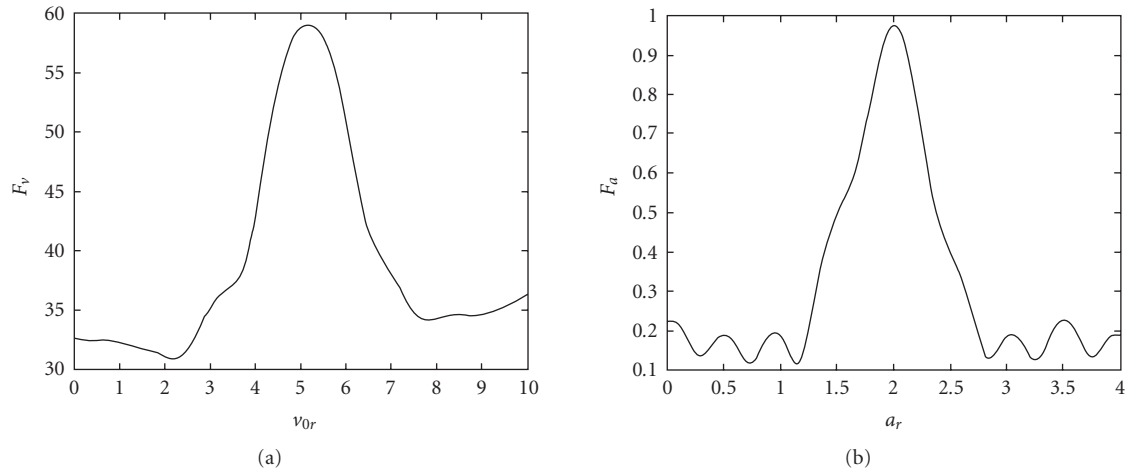


Figure 5: Plots of objective functions against the estimated parameters (a) $F_v$ versus $v_{0r}$ ($a_r = 2\,\text{m/s}^2$) and (b) $F_a$ versus $a_r$ ($v_{0r} = 5.15\,\text{m/s}^2$).

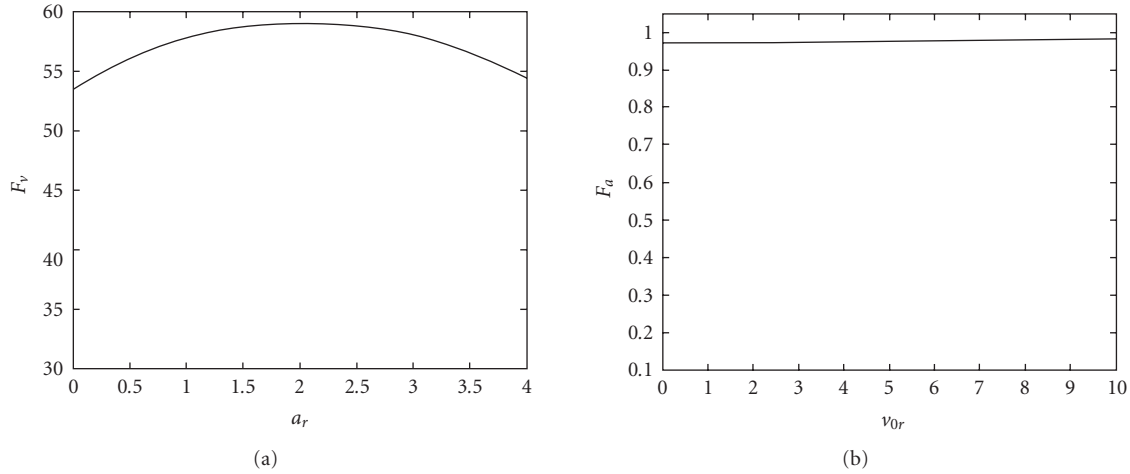


FIGURE 6: Plots of objective functions against the fixed parameters (a) $F_v$ versus $a_r$ ($v_{0r} = 5.15\,\text{m/s}^2$) and (b) $F_a$ versus $v_{0r}$ ($a_r = 2\,\text{m/s}^2$).

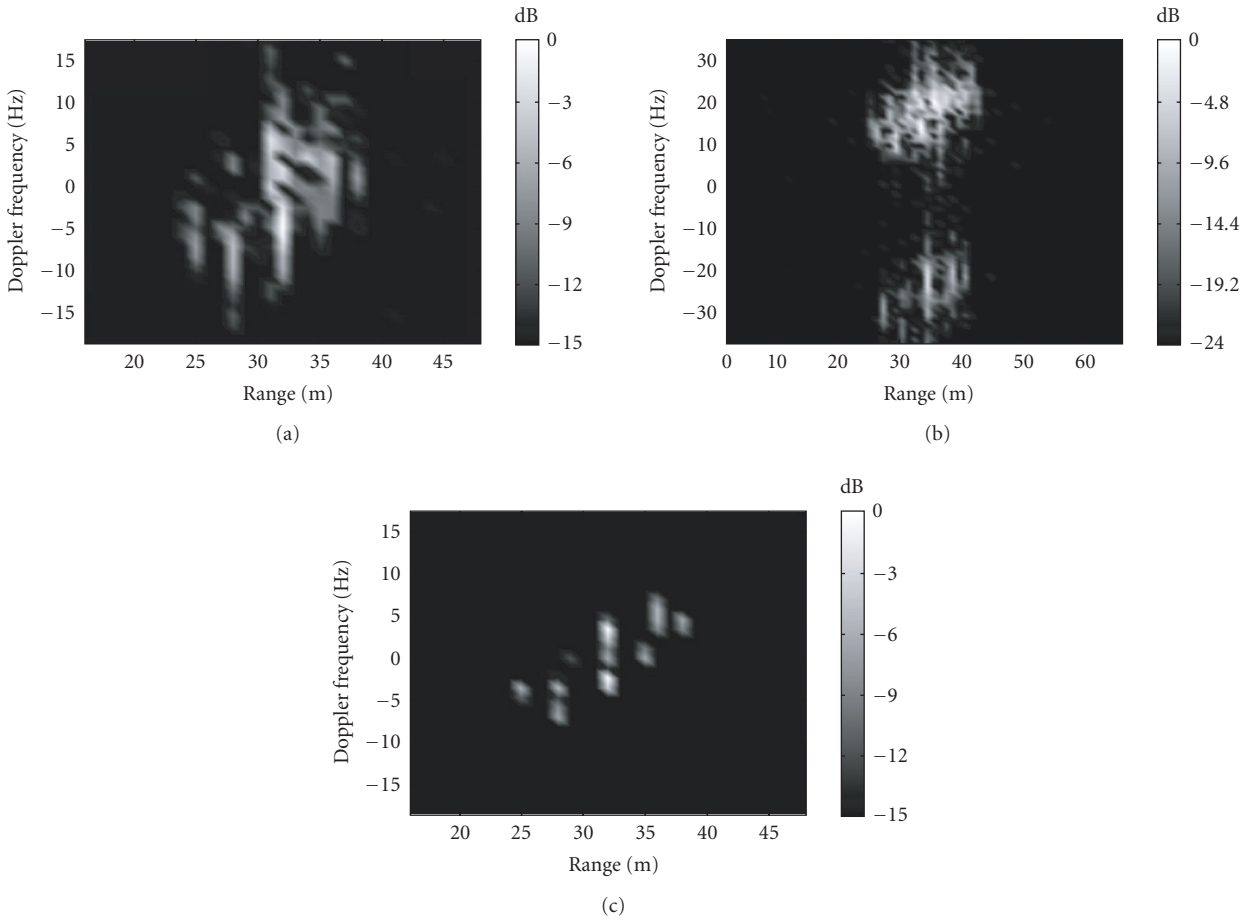


FIGURE 7: Range-Doppler image of simulated target (SNR = 10) using (a) MSA technique [5]; PGA technique [8]; (c) proposed subspace technique.

Figure 8: Schematic of a Boeing 737 (top view).

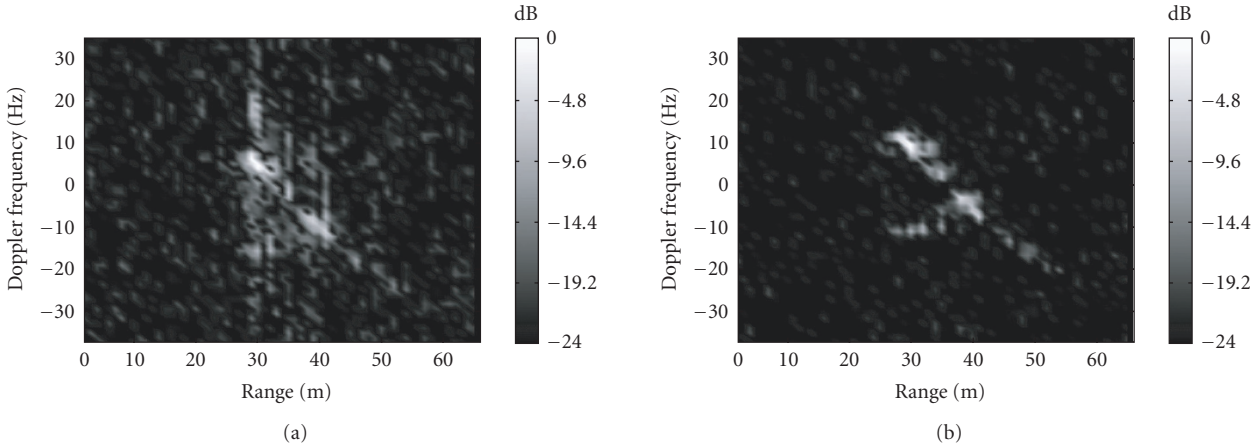


Figure 9: ISAR image of a Boeing 737: (a) MSA technique [5] (3 reference cells used); (b) proposed subspace technique.

## REFERENCES


[1] C.-C. Chen and H. C. Andrews, "Target-motion-induced radar imaging," *IEEE Transactions on Aerospace and Electronic Systems*, vol. 16, no. 1, pp. 2–14, 1980.

[2] G. Wang and Z. Bao, "The minimum entropy criterion of range alignment in ISAR motion compensation," in *Proceedings of the IEEE International Radar Conference*, pp. 236–239, Edinburgh, UK, October 1997.

[3] B. D. Steinberg, "Microwave imaging of aircraft," *Proceedings of the IEEE*, vol. 76, no. 12, pp. 1578–1592, 1988.

[4] W. C. Carrara, R. S. Goodman, and R. M. Majewski, *Spotlight Synthetic Aperture Radar: Signal Processing Algorithms*, Artech House, Boston, Mass, USA, 1995.

[5] B. Haywood and R. J. Evans, "Motion compensation for ISAR imaging," in *Proceedings of Australian Symposium on Signal Processing and Applications (ASSPA '89)*, pp. 113–117, Adelaide, Australia, April 1989.

[6] H. Wu, D. Grenier, G. Y. Delisle, and D.-G. Fang, "Translational motion compensation in ISAR image processing," *IEEE Transactions on Image Processing*, vol. 4, no. 11, pp. 1561–1571, 1995.

[7] E. Attia, "Self-cohering airborne distributed arrays on land clutter using the robust minimum variance algorithm," in *Proceedings of IEEE Antennas and Propagation Society International Symposium (APS '86)*, vol. 24, pp. 603–606, June 1986.

[8] D. E. Wahl, P. H. Eichel, D. C. Ghiglia, and C. V. Jakowatz Jr., "Phase gradient autofocus—a robust tool for high resolution SAR phase correction," *IEEE Transactions on Aerospace and Electronic Systems*, vol. 30, no. 3, pp. 827–835, 1994.

[9] F. Berizzi and G. Corsini, "Autofocusing of inverse synthetic aperture radar images using contrast optimization," *IEEE Transactions on Aerospace and Electronic Systems*, vol. 32, no. 3, pp. 1185–1191, 1996.

[10] L. Xi, L. Guosui, and J. Ni, "Autofocusing of ISAR images based on entropy minimization," *IEEE Transactions on Aerospace and Electronic Systems*, vol. 35, no. 4, pp. 1240–1252, 1999.

[11] H. Wu, D. Grenier, G. Y. Delisle, and D.-G. Fang, "Translational motion compensation in ISAR image processing," *IEEE Transactions on Image Processing*, vol. 4, no. 11, pp. 1561–1571, 1995.

[12] Y. Wang, H. Ling, and V. C. Chen, "ISAR motion compensation via adaptive joint time-frequency technique," *IEEE Transactions on Aerospace and Electronic Systems*, vol. 34, no. 2, pp. 670–677, 1998.

[13] F. Berizzi, E. Dalle Mese, and M. Martorella, "Performance analysis of a contrast-based ISAR autofocusing algorithm," in *Proceedings of the IEEE International Radar Conference*, pp. 200–205, Long Beach, Calif, USA, April 2002.
[14] J. Li, R. Wu, and V. C. Chen, "Robust autofocus algorithm for ISAR imaging of moving targets," *IEEE Transactions on Aerospace and Electronic Systems*, vol. 37, no. 3, pp. 1056–1069, 2001.
[15] F. Berizzi, M. Martorella, B. Haywood, E. Dalle Mese, and S. Bruscoli, "A survey on ISAR autofocusing techniques," in *Proceedings of IEEE International Conference on Image Processing (ICIP '04)*, vol. 1, pp. 9–12, Singapore, October 2004.
[16] D. A. Ausherman, A. Kozmer, J. L. Walker, H. M. Jones, and E. C. Poggio, "Developments in radar imaging," *IEEE Transactions on Aerospace and Electronic Systems*, vol. 20, no. 4, pp. 363–400, 1984.

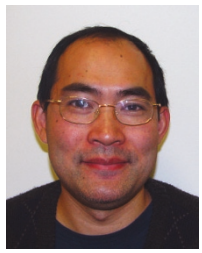

**D. Yau** received the B.E. degree in electrical engineering from The University of Sydney, Sydney, Australia, and the M.Eng.Sc. and Ph.D. degrees in electrical engineering from The University of Queensland, Queensland, Australia. He is currently working as a Research Scientist at DSTO, Australia. His research interests include radar imaging and signal processing.

**P. E. Berry** works in the Electronic Warfare and Radar Division of DSTO and has interests in estimation, optimization, and control applied to microwave radar engineering. He has previously worked in research laboratories in the UK's electricity supply industry on problems of computational physics and power system optimization and control.

**B. Haywood** received a Bachelor of Engineering (with honours) degree in 1984 and a Master of Engineering Science degree in 1988, both from the James Cook University, North Queensland Townsville. In 1988, he started studying for a Ph.D. degree at the University of Newcastle, NSW, which he was awarded in 1992. Since 1988, he has been with the Electronic Warfare and Radar Division (and its predecessors) of the Defence Science and Technology Organisation (DSTO) at Edinburgh, where he now holds the position of Head of Radar Modelling and Analysis and leads a group of engineers and scientists conducting research into airborne and surface-based radars operating in the maritime environment. He is a Member of the Institute of Electrical and Electronic Engineers (IEEE). His research interests include digital signal processing, high-resolution radar imaging (SAR and ISAR), automatic target recognition, and radar performance modelling.